www.maajournal.com

Mediterranean Archaeology and Archaeometry
Vol. 23, No 2, (2023), pp. 71-87
Open Access. Online & Print.

DOI: 10.5281/zenodo.7918170

PRELIMINARY PHYSICAL-CHEMICAL CHARACTERIZATION OF ARCHAEOLOGICAL METAL ARTIFACTS FROM POLICORO AREA (MATERA, SOUTHERN ITALY)

Nicoletta Sgarro[1], Savino Gallo[2], Ernesto Mesto[3], Giovanna Rizzo[1], Laura Scrano[4], Gioacchino Tempesta[5]

[1]Dipartimento di Scienze, Università della Basilicata, Via dell'Ateneo Lucano 10, Potenza, Italy
[2]Direttore del Museo Archeologico Nazionale della Siritide, Via Colombo, 8 75025 Policoro (MT), Italy
[3]Dipartimento di Scienze della Terra e Geoambientali, Università degli studi di Bari Aldo Moro, Via Edoardo Orabona, 4, 70125 Bari BA, Italy
[4]Dipartimento delle Culture Europee e del Mediterraneo, Università della Basilicata, Via Lanera, 20, 75100 Matera MT, Italy
[5]Dipartimento Geomineralogico, Università degli Studi di Bari, Via Edoardo Orabona, 4, 70125 Bari BA, Italy

Received: 27/04/2023
Accepted: 05/06/2023

Corresponding authors: Giovanna Rizzo (giovanna.rizzo@unibas.it); Laura Scrano (laura.scrano@unibas.it)

ABSTRACT

This study aimed to characterize seven metal artifacts found during archaeological excavations in the Siris area of Policoro (Matera, Southern Italy) dated during the five centuries BC. A range of analytical techniques, including optical microscopy (OM), X-ray fluorescence (XRF), X-ray diffraction (XRD), and X-ray photoelectron spectroscopy (XPS), were applied, and a microbiological investigation was performed. Visually, the metal finds appeared to be deteriorating from severe corrosion. The state of oxidation, evidenced through OM on the surface of a lead stick and an arrowhead, did not allow the recognition of the constituent materials, which were qualitatively obtained by XRF and, in the case of an arrowhead by XPS. On the other hand, the XRD technique was decisive in characterizing a lancet. The XRF application was only possible for a fibula, a flask cap, an iron weapon, and a javelin tip, which allowed the first characterization of these metal finds. The acquired information is crucial to evaluate a suitable green protocol in the study's second phase to recover and preserve these artifacts as better as possible.

KEYWORDS: corrosion, biological deterioration, green protocols, Siris area, Southern Italy, Fibula, XRF, XPS, XRD, arrowhead

1. INTRODUCTION

Art and science were considered for a long time, separated entities (Avilia, 1980). Yet, according to Thucydides, archaeology is very important because it aims to demonstrate and shape the "history" of found archeological artifacts (Parmeggiani, 2003; https://euro-acad.eu/events?id=140).

Some authors (Artioli, 2010; Iacopini, 2012;) report that people from ancient cultures knew only eight elements: copper (Cu), lead (Pb), tin (Sn), zinc (Zn), iron (Fe), gold (Au), silver (Ag) and mercury (Hg); less commonly used but probably known elements were antimony (Sb) and platinum (Pt).

Among the metals mentioned, only silver, iron, gold, platinum, and copper exist in nature in their native state or as pure elements. In contrast, the other elements combined to form oxides and sulphides (Cabibbo, 2018).

The use of metals over the years implies that mining and processing techniques were known in the past; therefore, the discovery of metals is directly linked to people's evolution, with the production of weapons, agricultural tools, and work objects influencing the life of every day.

Determining the elements that make up the alloys of archaeological metal artifacts is essential to acquire information about the historical and geological placement of the sample under examination (Aceto, 2005).

Non-destructive techniques such as optical microscopy (OM), X-ray diffractometry (XRD), and X-ray photoelectron spectroscopy (XPS), and X-ray fluorescence (XRF) have been widely applied to metallic archaeological artifacts to understand their raw materials and evaluate the corrosion phenomena (Mircea et al., 2012; Brocchieri et al., 2022). The non-destructive characteristics of XRF are particularly suitable for research in archaeological heritage, where the sample is unique, or its integrity has technical or significant features from a historical point of view. In museum analysis, XRF analysis allows you to identify the raw materials and metal alloys, and provide the characterization of objects such as jewelry, silverware and weapons, thus assisting conservators in the conservation and restoration of artifacts (Liritzis et al., 2018).

The main objective of these investigations is to preserve the archaeological artifact for the next generations, especially when they come to works of art that are part of the cultural heritage (Kylafi et al., 2017; Muşkara and Aydýn, 2022).

Metal artifacts, with time, are subjected to undergo corrosion processes. The definition of corrosion given by the International Organization for Standardization (ISO) is "physicochemical interaction between a metal and its environment, which results in changes of the metal properties and may often lead to impairment of its function, the environment, or the technical system of which it forms a part". IUPAC (the International Union of Pure and Applied Chemistry) also gives a broader definition of corrosion, including the degradation of non-metals as well as metallic materials: Corrosion is an irreversible interfacial reaction of a material (metal, ceramic, and polymer) with its environment, which results in consumption of the material or dissolution into the material of a component of the environment. Often, but not necessarily, corrosion results in effects detrimental to the usage of the material considered. Exclusively physical or mechanical processes such as melting or evaporation, abrasion or mechanical fracture are not included in the term corrosion" (IUPAC, 2014).

The study of the deterioration of metal finds, which can be influenced by a series of parameters, including the surrounding environment, is substantial for the history of the analyzed material.

The deterioration can also be of a biological type and manifest itself for an extended period, even in non- extreme environmental conditions with the presence, for example, of molds and parasites that cause rapid, severe, and irreversible degradation (MacLeod, 1991; Videla, 2002; Bouchard et al., 2003; Frost, 2003; Giumlia-Mair, 2005; Ingo et al., 2006; Figueiredo et al., 2007; Bernard et al., 2009; Mata et al., 2009; Campanella et al., 2009; Corsi et al., 2016; Balassone et al., 2018).

The biological corrosion process requires the presence of three elements: the metal, the electrochemical solution, and the microorganisms. Compared to corrosion not influenced by microorganisms, its peculiar characteristic lies in the fact that the latter can initiate, facilitate or accelerate the corrosion reactions electrochemistry occurring on the surface of the metal, leading to the degradation of the material. Microbiological corrosion can occur both locally and in the form of pitting. In general, the specific process depends on the metal substrate and the environment in which it is located (Videla, 2002). In contact with air, humidity, and carbon dioxide, an external layer spontaneously forms on the product, with a protective effect for the underlying material, and a surface layer called patina forms on the surface of the metal products (Chiavari et al., 2006; Robbiola et al., 2008).

The present study aims to determine the physical, chemical, and biological characteristics of some selective archaeological metal artifacts saved in the National Archaeological Museum of the Siritide (Policoro, Italy). They were found during archaeological excavations in the Siris area, an ancient settlement of Magna Graecia. This area is located on the Gulf of Taranto between the rivers Aciris (modern Agri) and Siris (modern Sinni) in the territory of Policoro's Municipality in the Province of Matera, Basilicata, Italy.

The chemical-physical characterization of metallic materials turned out to be preparatory for a second phase of the project, which will deal with non-destructive restoration and conservation techniques that could be adopted to save the metal finds best.

2. SAMPLING STRATEGY AND ANALYTICAL TECHNIQUES

2.1 Sampling

A set of seven metal artifacts found during archaeological excavations in the Policoro area (Basilicata), housed in the National Archaeological Museum of the Siritide, was subjected to non-destructive chemical, physical and biological characterization (Table 1).

Policoro is located in the Metapontum plain, on the Gulf of Taranto at South of Italy (Fig.1).

It lies between the mouth of the Cavone River and the settlement of Marina di Ginosa in the southeastern territory of the Basilicata region along the Ionian coast. It includes the final stretch and the mouth of the Sinni River. The area of Policoro falls within a sector of the Fossa Bradanica where "terraced marine deposits" or "deposits of terraced coastal prisms" of the Middle-Upper Pleistocene age (1.5-0.12 Ma) emerge, resting on sub-Apennine clays, sandy, sandy-gravelly and sandy-silty deposits of the alluvial and coastal plains of the Holocene age (Pescatore et al., 2009; Sabato et al., 2011) (Fig. 2).

Figure 1. Location of Policoro (image given on Google Earth on 15.05.2023)

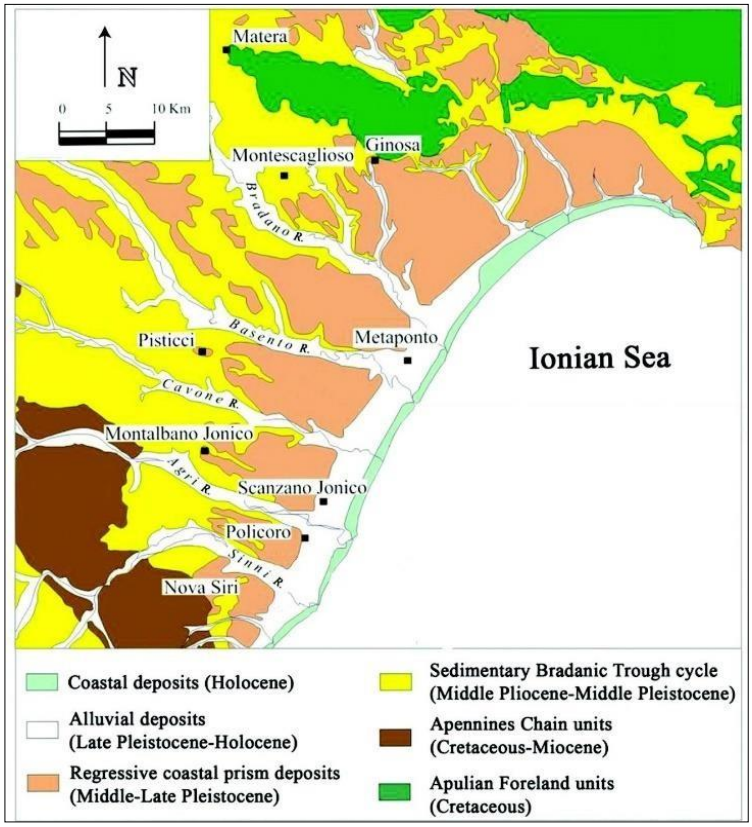

Figure 2. Schematic geological map of the Bradanica trench sector. Sheet No. 508 "Policoro" (modified after Pescatore et al., 2009; Sabato et al., 2011).

A set of seven archaeological artifacts (Table 1, Fig. 3) was chosen based on some special factors including the typological representativeness of the contexts of use, and of the places where these objects were found and based on the raw materials used to forge the artifacts. They provide a wider picture of the types of materials that came from and used in Magna Graecia between the 5th and 2nd century BC.

Unfortunately, the Museum's conservation policy of extracting samples from the completely preserved artifacts was not possible. Consequently, the application of analytical techniques was also limited to a few non- destructive ones.

Table 1. Archaeometric identification of metal artifacts collected from the Policoro area.

Sequence	Identification code	Artifact	Dating	Archeological context	Excavations places	Size (cm)
a	207559	Javelin tip for battle	IV sec. B.C.	Necropolis context	St. Arcangelo	length: 14 thickness: 0.6 – 2.5
b	216346	Iron weapon	IV-II sec. B.C.	Sacral context	Demetra sanctuary	length: 14 thickness: 0.3
c	46382	Lead stick	VII sec. B.C.	Votive offer	Siris acropolis	length: 5
d	46995	Flask cap	V sec. B.C.	Funerary context	Siris, western necropolis	diameter: 2.4
e	35207	Arrowhead	IV-I sec. B.C.	Housing context	Herakleia acropolis	length: 2.5
f	38747	Fibula	Unknown	Votive offer	Siris archaic temple	length: 5 thickness: 0.5 – 1.0
g	35514	Lancet	IV-I sec. B.C.	Housing context	Herakleia acropolis	length: 12.9

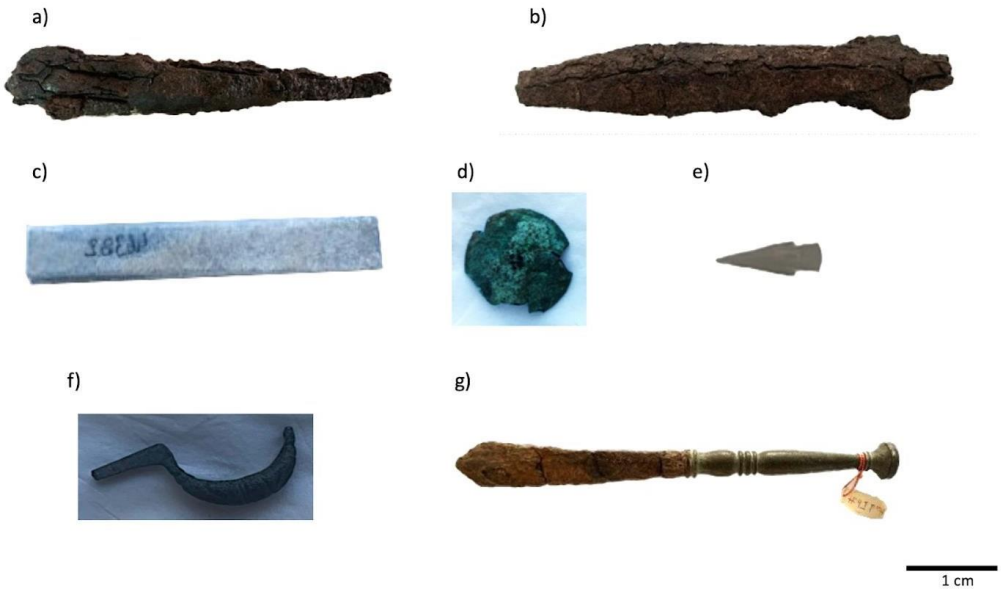

Figure 3. Studied archaeological metal finds; a) javelin tip for battle; b) iron weapon; c) lead stick; d) flask cap; e) arrowhead; f) fibula; g) lancet.

2.2 *Analytical techniques*

The samples were examined using various analytical techniques, such as Optical microscopy (OM), X-ray fluorescence (XRF), X-ray diffraction (XRD), and X-ray photoelectron spectroscopy (XPS), to determine the chemical and physical characteristics of artifacts. The use of these techniques becomes important because it provides a lot of information regarding the raw materials that lead to an understanding of the social and economic history of these artifacts (Mazzeo, 2012; Salem, 2021; Rifai, 2023). The choice of analytical techniques was guided by the need to avoid damaging the selected objects. However, due to the studied samples' size, carrying out all the listed instrumental diagnostic analyses on each artifact was impossible. A list of the possible analytical techniques for each piece is reported in Table 2.

A biological approach was also performed on metal objects to determine the presence of degradation microorganisms (Lekbach et al., 2021).

2.3 *Optical Microscopy (OM)*

The arrowhead and the lead stick were exanimated at the University of Calabria (Arcavacata di Rende, Cosenza, Italy) using the Dinolite AM4113TFVW Portable Digital Optical Microscope. The analyses were performed using visible light and UV LEDs with a magnification of 50 units of measure (actual size of about 7 mm) and 200 units of measure (actual size of about 2 mm), respectively.

This instrument has a resolution of 1.3 Mpixel, and a magnification range of 10 ×,÷ 50 × and 200 ×; and features 4 UV LEDs with 400nm+ emission and 4 built-in white LEDs, with a frame rate of more than 30 fps. The sensor is a color CMOS, with manual calibration and measurement accuracy of approximately ±3µm.

2.3.1 X-ray diffractometry (XRD)

The lancet (Fig. 2g) underwent XRD analysis using a PANalytical Empyrean diffractometer at the Earth and Geoenvironmental Sciences Department of Bari University (Italy). The instrument operated at 40 kV/40 mA in Bragg-Brentano geometry and was equipped with a nickel-beta filter, CuKα radiation, and a PIXcel3D detector (Malvern PANalytical, Almelo, The Netherlands). Phase identification was performed using the PANalytical B.V. software HIGHScore Plus version 4.6a (Malvern PANalytical, Almelo, The Netherlands).

2.3.2 X-ray photoelectron spectroscopy (XPS)

XPS provides a complete elemental analysis, except for hydrogen and helium, of the first 10–200 Å layer (depending on the sample and instrumental conditions) of any solid surface stable under vacuum or can be made vacuum stable by cooling. Information on chemical bonding is also provided. Of all the instrumental techniques currently available for surface analysis, XPS is generally considered the quantitative, easily interpretable, and informative concerning chemical information. For these reasons, it was highly recommended (Pintori et al., 2022).

XPS was used to analyse the arrowhead at the University of Basilicata (Potenza, Italy). The instrument is a double anode XPS PHOIBOS 100-MCD5 spectrometer (Mg Kα and Al Kα). The spectrometer is equipped with a multi-channel detector that allows working at high lateral resolution (and in energy),

maintaining high sensitivity in the electronic counting. The spectra were acquired with the Mg Kα (1253.6 eV) source operating at 10 kV and 100 mA in 'medium area' mode with a lateral spot of approx. 2 mm. Peaks areas and positions (binding energies, BE) as derived by the curve-fitting were normalized using proper sensitivity factors and referenced to C1s aromatc/aliphatic carbons as the internal standards were set at 284.8/285.0 eV (Briggs, 1990; Matthew2004).

2.3.3 X-ray fluorescence (XRF)

The analyses were performed on the javelin tip (Fig. 2a), iron weapon (Fig. 2b), flask cap (Fig. 2d), fibula (Fig. 2f), and lancet (Fig. 2g) with an assembled portable XRF instrument at the University of Bari (Bari, Italy). The X-ray source is an AMPTEK (Inc. USA) Mini-X with Au target, operating at 40 kV and 95 µA. The detector is a silicon drift (SDD) Amptek XR-123 SDD with a 25 mm2 detection area, 500 µm thickness (fully depleted), and a 12.5 µm Be window. Resolution at 5.9 keV is 135 eV at room temperature. The system is equipped with two laser pointers to identify the central point of the X- ray beam at a 90° angle from the detector axis. This geometry allows partially polarized radiation with a high background reduction on Compton scattering.

Samples were analyzed directly on air at room temperature. The outgoing radiation is collimated in a 5 mm beam diameter at the sample surface. Each acquisition had a fixed working distance (15 mm) between the instrument and the parchment surface controlled by a laser interferometer. The acquisition time for each spectrum was 60 s. The spectra for qualitative analyses were collected and elaborated with the software Surface Monitor 7.0 (by Assing Spa). XRF analysis in the air generates some physical limits in lighter elements detection. In our case, only elements with Z equal to or higher than 16 (S) were detectable with the previously described setup. Instead, to analyse the arrowhead and lead stick was used the portable XRF instrument (Avarcata di Rende, Cosenza). With the system used, the detection of fluorescence in the sample is recorded by a solid-state detector SDD (Silicon Drift Detector) which allows to the identification of all the detectable elements in the sample in a single measurement. For energy dispersion analysis a portable spectrometer is used which exploits low-power x-ray tubes and detectors which do not require cooling with liquid nitrogen, coupled with a portable computer.

The portable XRF spectrometer, used to carry out the above analyses, consists of: an X-ray tube (Mini-X - Amptek) with a maximum voltage of 40 kV, maximum current 0.2 mA, target in Rhodium (Rh), dedicated control software; an SDD system for the detection of the secondary detection emitted by the sample (X-123SDD – Amptek) with resolution 125 - 140 eV FWHM @ 5.9 keV; energy detection range: 1 keV - 40 keV; maximum content rate up to 5.6 x 105 cps; dedicated control software. For the acquisition of the X-ray fluorescence signal of the selected measurement areas in the two metal finds, the following measurement parameters were used: voltage, 35 kV; current, 80µA; acquisition time 50 seconds for the measured area, working distance from the surface 1 cm.

2.3.4 Biological approach

Sampling and isolation of the bacterial strains collected on the surfaces of the metal finds was carried out according to the Recommendation of the Ministry of Cultural Heritage n.3/1980, using sterile and dry swabs. Subsequently, biological samples were isolated, dissolving in 500 µL of sterile Ringer's solution, vortexing for 10 minutes, and pipetting a 100 µL aliquot into 5 mL of Plate Count Broth (PCB); after 24 hours of incubation at 30°C, the culture was used for inoculation on Plate Count Agar (PCA) plates, which were further incubated at 30°C for seven days. Then the plates were observed using a standard light microscope to check for the presence of biological colonizers on the metallic material.

The biological analysis did not reveal the presence of microorganisms. Since the Museum usually exhibited the metal finds to the public, they had probably been subjected to cleaning by using disinfectants. Therefore, we could not state if their visible corrosion derives from a microbiological deterioration or is due to other environmental issues that arose in the archaeological site of origin. For this reason, the biological data are not discussed in the following sections.

3. RESULTS AND DISCUSSION

Table 2 shows the non-destructive analyses performed for each artifact. Only XRF was applied to the whole set of metal finds selected by the Museum.

Table 2. Diagnostic analysis performed on the artifacts.

Sequence	Artifact	OM	XRD	XRF	XPS
a	Javelin tip for battle			X	
b	Iron weapon			X	
c	Lead stick	X		X	
d	Flask cap			X	
e	Arrowhead	X		X	X
f	Fibula			X	
g	Lancet		X	X	

OM Optical microscopy; XRD X-ray diffractometry; XRF X-ray fluorescence; XPS X-ray photoelectric spectroscopy.

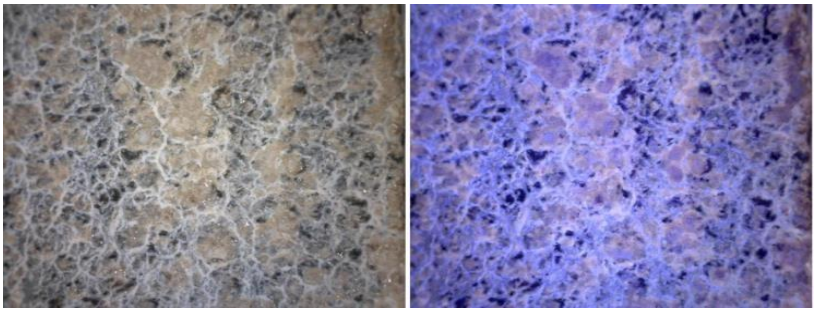

A B

Figure 4. Optical microscopy analysis of the lead stick (50 units magnification (7 mm); [A] visual and [B] UV pictures.

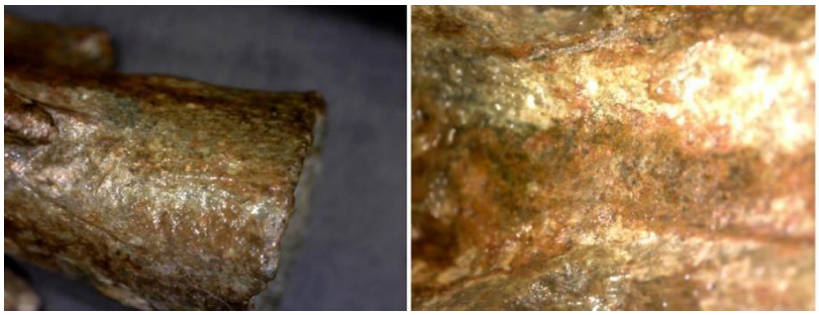

A B

Figure 5. Optical microscopy analysis of the arrowhead, [A] 50 (7mm) and [B] 200 units (2 mm) vis. magnifications.

3.1 Optical Microscopy (OM)

This technique provided information about the physical structure of the metal finds (Moropoulou et al., 2013). Figures 4 and 5 depict the lead stick and arrowhead surface obtained by OM.

The observation of the samples via OM suggested the presence of multiple layers made of organic materials and oxidized metal. The artifacts appeared highly deteriorated, perhaps due to the environment in which they were found. The state of corrosion shows a granular appearance, but for the arrowhead, it is difficult to recognize the native surface state of the artifact.

3.1.2 XRF, XPS, and XRD features

The appearance due to the corrosion and oxidation phenomena did not allow for the visually recognizing of the component materials. While with the help of the XRF application, it was possible to detect all the elements of the alloy used for each studied sample and have an idea of its main component (Table 3).

Table 3. Elements and materials of the artifacts

Sequence	Artifact	Identification code	Ca	Ti	Mn	Fe	Cu	Zn	Sn	Pb	Material
a	Javelin tip for battle	207559	X	-	tr	X	tr	tr	-	-	Iron
b	Iron weapon	216346	tr	-	-	X	tr	-	-	-	Iron
c	Lead stick	46382	tr	-	-	-	-	-	-	X	Lead
d	Flask cap	46995	tr	-	-	tr	X	tr	X	tr	Bronze
e	Arrowhead	35207	tr	-	-	tr	X	-	X	X	Copper
f	Fibula	38747	tr	tr	-	tr	X	tr	X	tr	Bronze
g	Lancet blade	35514	tr	-	-	X	tr	tr	-	-	Iron
	Lancet handle		tr	-	-	tr	X	X	X	tr	Brass

X: main element; tr: traces

3.2 *Javelin tip for battle*

The XRF results (Figure 6) obtained for the javelin tip (Table 1, Figure 2a) highlighted iron as the main constituent and calcium that probably belongs to some exogenous alteration materials. Traces of other elements were also detected (Table 3).

3.3 *Iron weapon*

The iron weapon (Table 1, Figure 2b) evidenced a somewhat deteriorated appearance. The XRF analysis showed iron as its main component (Figure 7). Traces of Ca and Cu were also found (Table 3).

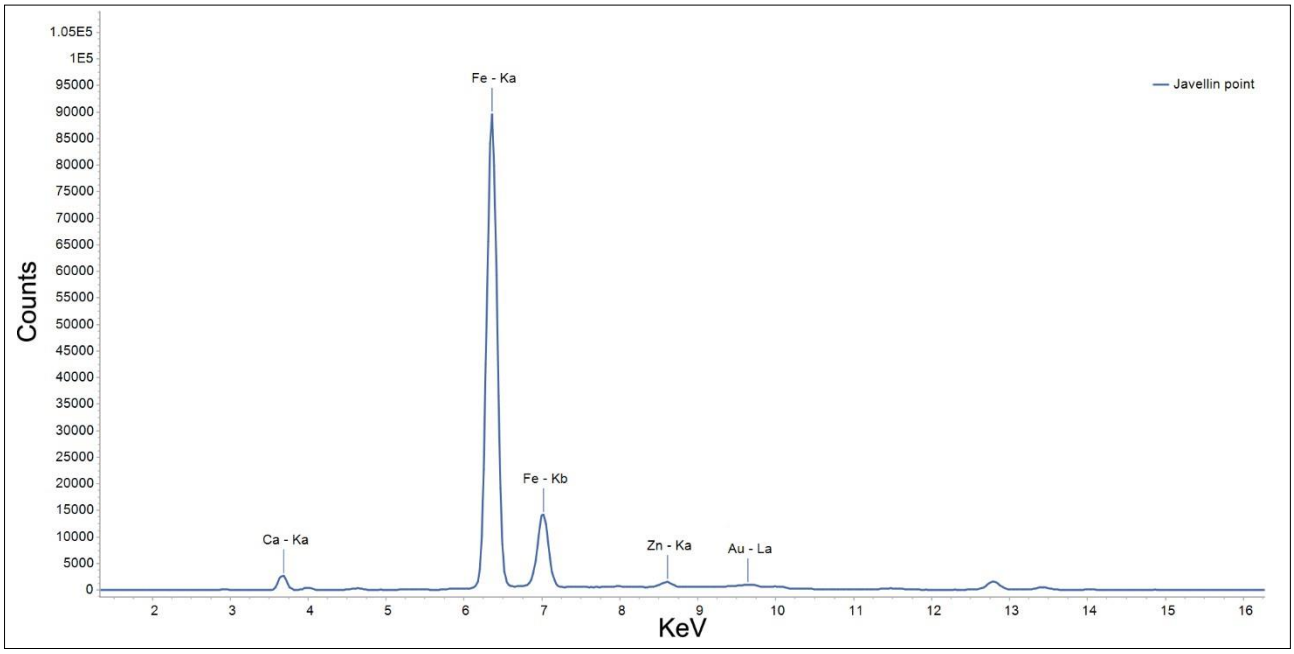

Figure 6. The X-ray fluorescence (XRF) analysis of the javelin point.

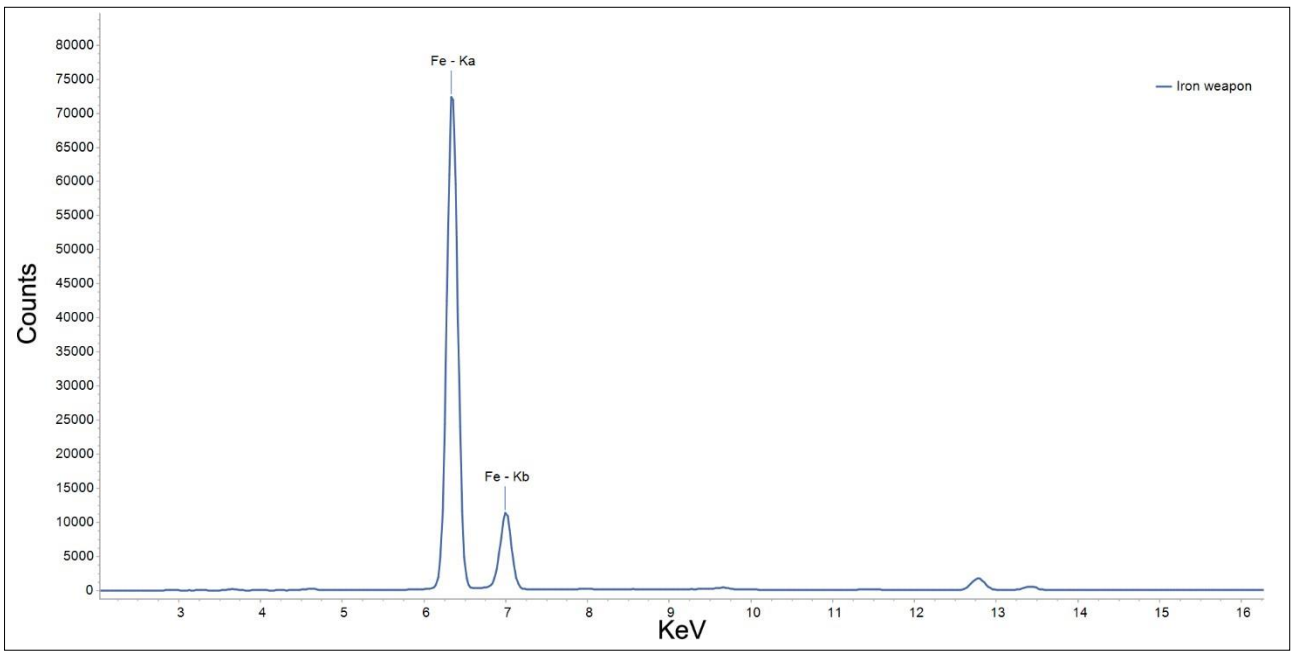

Figure 7. The X-ray fluorescence (XRF) analysis of the iron weapon.

3.4 *Lead stick*

The lead stick (Table 1, Figure 2c) examined is part of a set of 102 sticks contained inside an amphora (Figure 8) at the time of its discovery. They may have served as weights for shipping nets (Verger S., 2014). The stick is made of lead, showing severe degradation even with the naked eye.

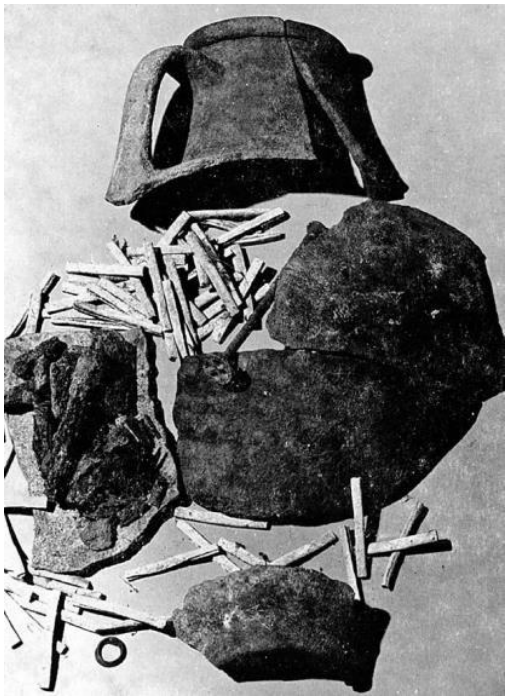

Figure 8. Amphora with 102 lead sticks

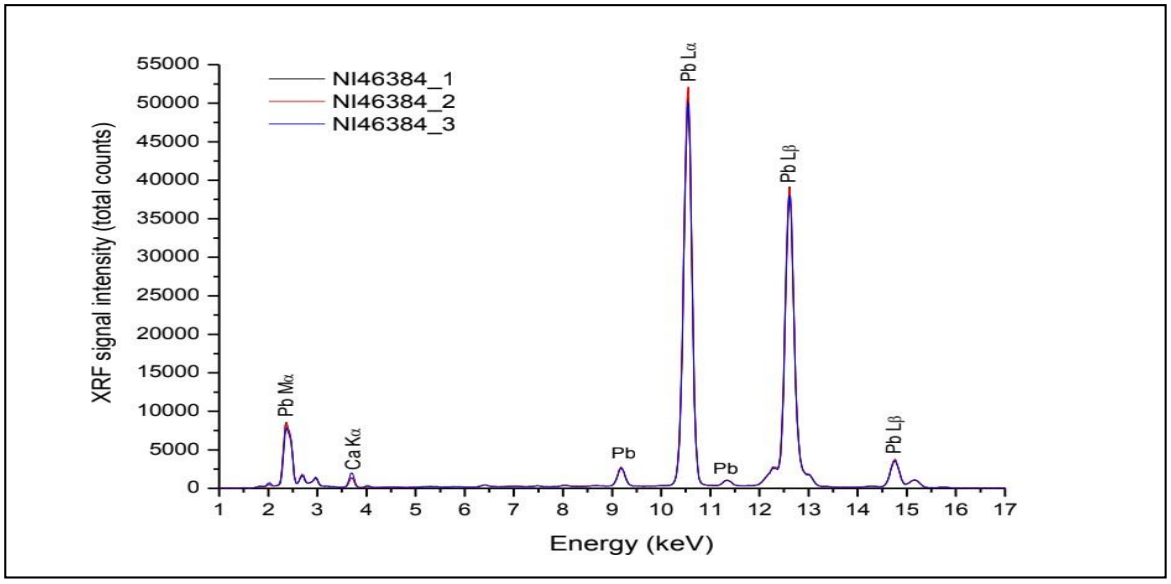

Figure 9. The X-ray fluorescence (XRF) analysis of the lead stick.

On this find, it was possible to carry out analyses with the portable OM (Fig. 4) and XRF (Fig. 9).

Also, in this case, traces of calcium due to natural contamination were evidenced by XRF (Table 3).

3.5 Flask cap

The flask cap (Table 1, Fig. 2d) already appeared to the naked eye deteriorated significantly. XRF analysis (Fig. 10) highlighted the presence of copper and iron as elemental components of the alloy and calcium as a contaminant (Table 3)

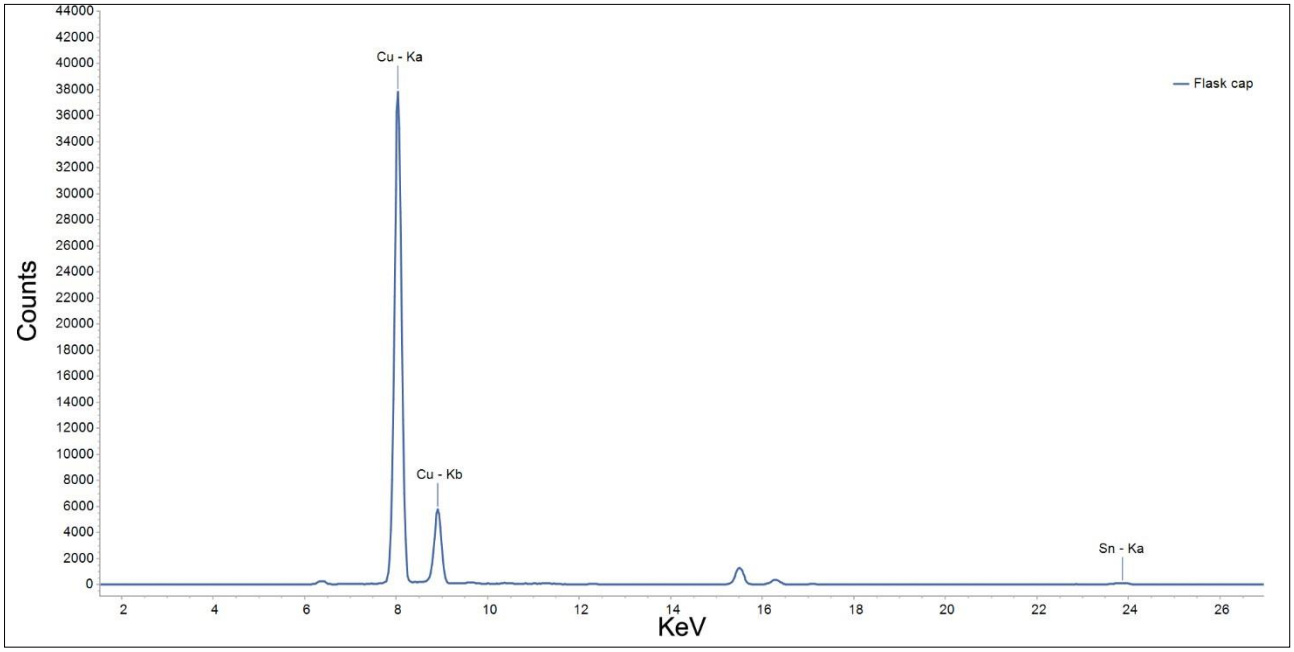

Figure 10. The X-ray fluorescence (XRF) analysis of the flask cap.

3.6 Arrowhead

XRF analysis of the arrowhead (Table 1, Fig. 2e) showed that copper (prevalent), nickel, lead (high), tin, zinc, and iron constitute the elemental composition of the alloy, and calcium is in the trace as a contaminant (Table 3, Fig. 11). The optical microscopy (Fig. 5) showed surface morphological alterations visible to the naked eye. The XPS analysis confirmed this deterioration state, highlighting the presence of oxidized chemical compounds (Fig. 12).

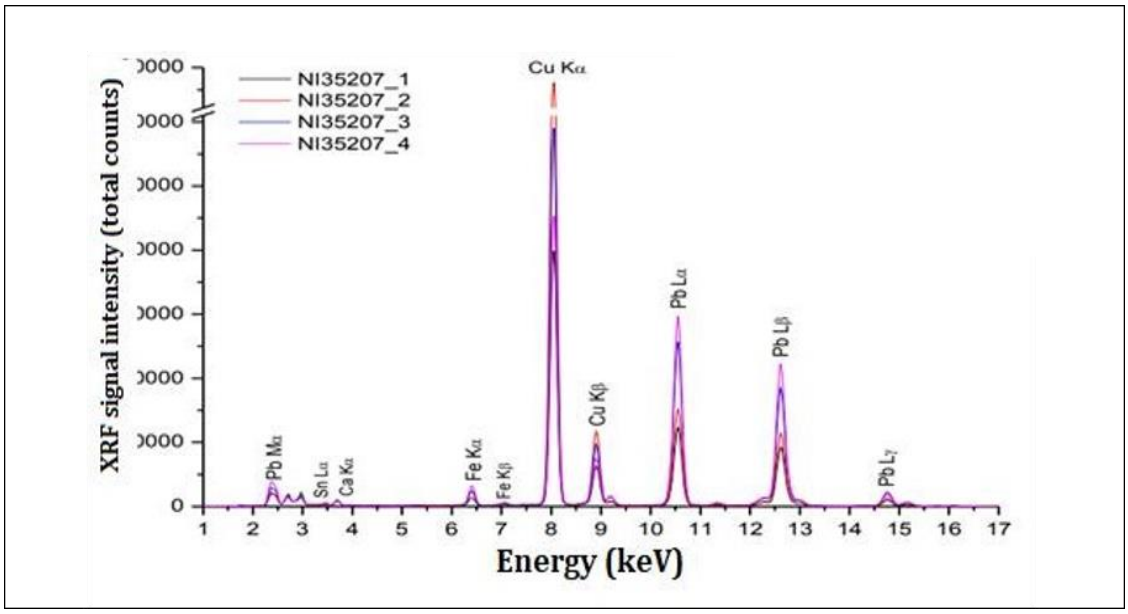

Figure 11. The X-ray fluorescence (XRF) analysis of the arrowhead.

The XPS analysis of the sample showed the presence of the following elements: carbon (C1s); oxygen (O1s); copper (Cu2p); nitrogen (N1s); calcium (Ca2p); lead (Pb4f); sulphur (S2p); silicon (Si2p); sodium (Na1s). The presence of chlorine (Cl2p) was only probable.

Aluminium (Al2p), if present, is covered by other secondary signals, while tin, if present, is covered in negligible quantities. Tin is a component of the bronze alloy together with copper.

Given the need to have some more information on the chemical form in which the lead is present, the BE (binding energy) of lead (Pb4f) was compared with those reported in the XPS NIST database (https://srdata.nist.gov/xps/main_search_menu.as

px). It should be noted that this information was obtained without fitting the C1s and Pb4f regions but from the observation of the spectra acquired as such. The Pb4f7/2 signal of the studied arrowhead falls at a BE of 139.5 eV, indicating PbC2O4, PbSO4, and Pb(NO3)2 as plausible chemical species. Widening the search interval to ± 1.0 eV, the species found, in addition to those already listed, were PbS, PbCl2, and Pb(C2H3O2)2.

As regards the presence of lead in the form of PbO2, a constituent of the mineral known as plattnerite, the values reported by the NIST database for lead in the form of oxide are PbO2 = 136.8 – 138.2 eV; PbO = 137.6 -138.2 eV; Pb3O4 = 137.8 eV.

As can be seen, the BE value of the various forms of lead oxide is more than one electron volt higher than the experimental value found. From this result, it can be assumed, with all the necessary precautions, that the lead found is probably not present in the form of oxide. The sample was analysed on a different side of the arrowhead, and checking for the Pb4f7/2 positions, the BE value was 139.1 eV; therefore, the result did not change so much by changing the analyzed side.

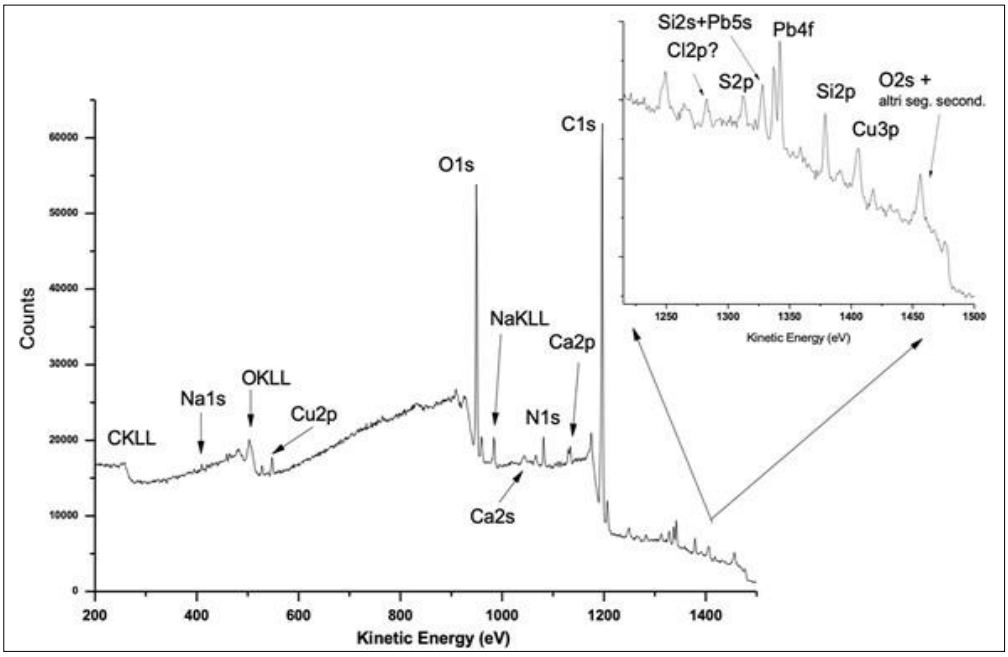

Figure 12. X-ray photoelectric spectroscopy (XPS) analysis of arrowhead.

3.7 Fibula

The XRF analysis of the fibula (Table 1, Figure 2f), showed that the main components were copper, tin, lead, iron, and calcium (Table 3, Fig.13). The latter element is a contaminant. The object appeared oxidized but still intact.

3.8 Lancet

Two XRF analyses had to be carried out on the lancet (Table 1, Fig. 2g) since the lancet blade and the handle appeared to be produced with different materials to the naked eye. The XRF analysis of the lancet blade (Table 3, Fig. 14) cleared that it was created with only iron as a raw material. In contrast, the XRF analysis of the lancet handle (Fig. 15) showed that it was produced with an alloy of copper, zinc, and iron (Table 3).

XRD analysis was performed on both the blade and the handle confirming the results obtained by XRF. The diffraction pattern generated by the blade (Fig. 16) revealed the occurrence of iron, aluminum, quartz, calcite, and analcime. In contrast, the X-ray pattern of the handle (Fig. 17) showed the presence of metallic iron and hydroxide, metallic and oxides copper, lead oxide, and quartz. The presence of two broad peaks centered at 2θ ~ 18° and 29°, respectively, indicates the presence of micro-crystalline graphite and an amorphous component on the blade.

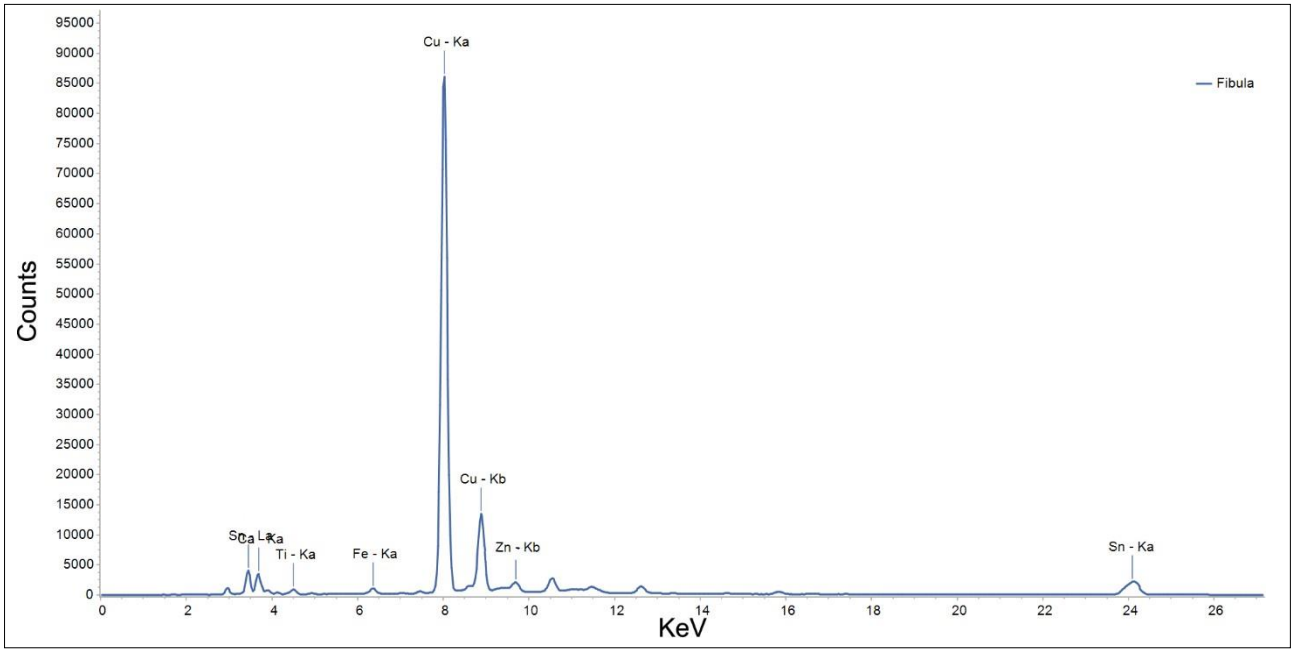

Figure 13. The x-ray fluorescence (XRF) analysis of the fibula.

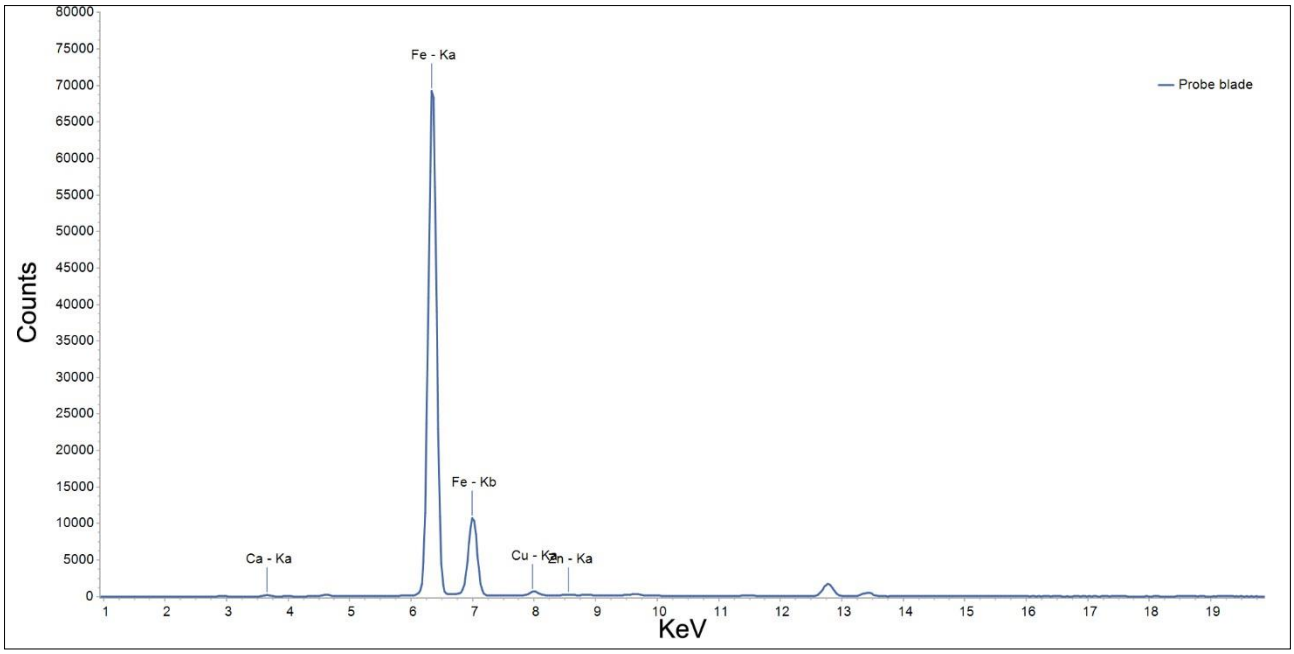

Figure 14. The x-ray fluorescence (XRF)analysis of the lancet blade.

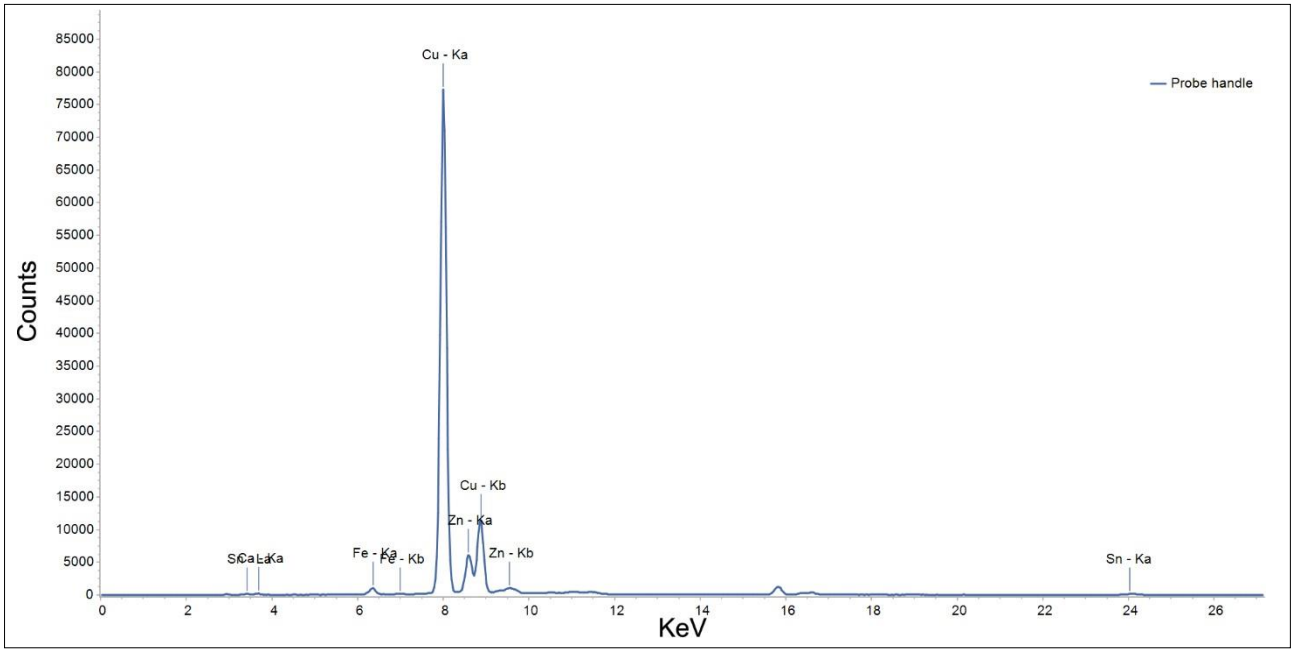

Figure 15. The x-ray fluorescence (XRF) analysis of the lancet handle.

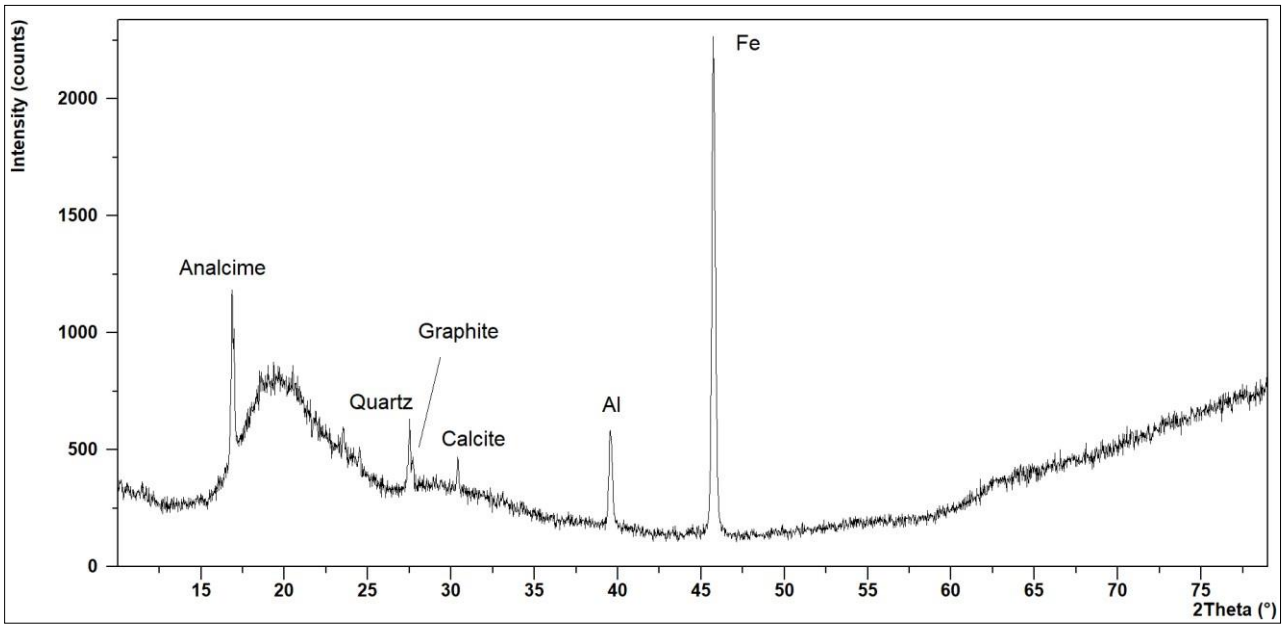

Figure 16. The X-ray diffraction (XRD) pattern of the lancet blade.

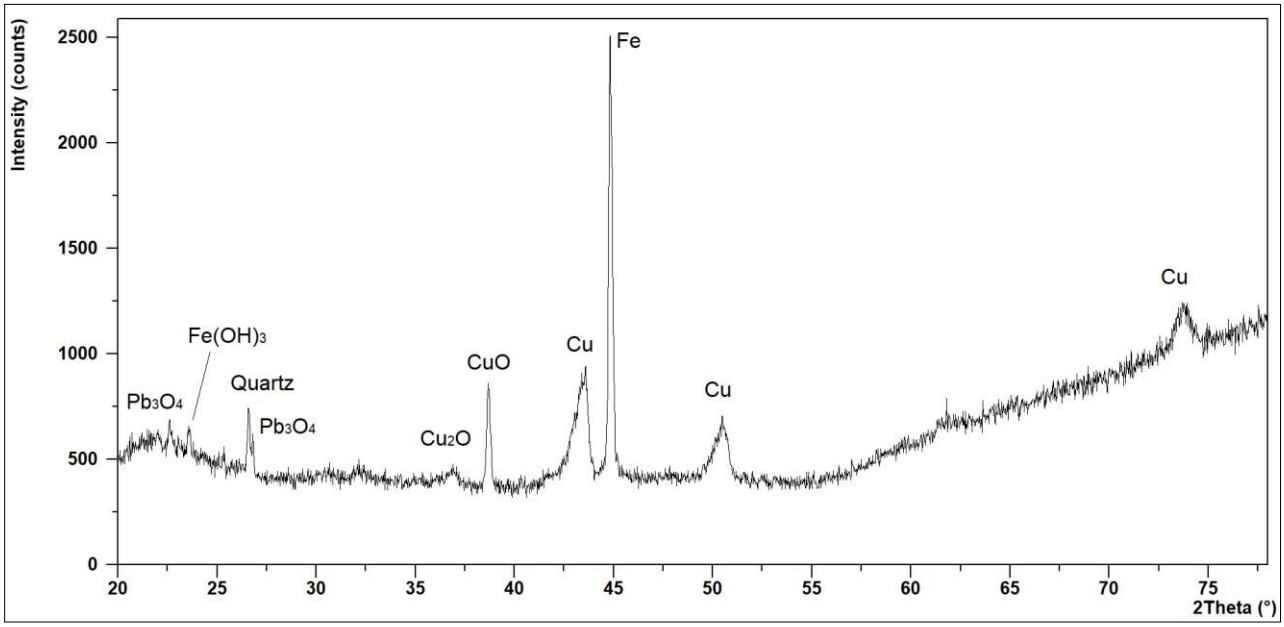

Figure 17. The X-ray diffraction (XRD) pattern of the lancet handle.

4. DISCUSSION & CONCLUSION

This study dealt with the instrumental characterization of some metal finds generously entrusted to us by the National Archaeological Museum of Sirtide - Policoro (MT).

Since the presence of specific chemical elements within the alloy of the artifact can considerably influence the effectiveness of their cleaning or consolidation treatments, we tried as far as possible to obtain a compositional analysis of their construction materials.

As the Museum's rules prevented the removal of the archaeological finds kept there for a long time, we used portable instruments, when available, and not for all metal objects. Anyway, XRF was applied for the characterisation of all the metal finds.

Iron was the main constituent of the javelin tip, iron weapon, and lancet blade. The alloy of the lancet handle was indeed brass for the presence of Cu, Zu, and Sn. The flask cap and fibula were bronze, with Cu and Sn as the main elemental constituent. Lead was the main constituent of the lead stick and was also present in the arrowhead with Sn and Cu. This last element was the principal substance for the arrowhead, emerging that the artifact, contrary to the information in the museum literature, was not made of iron but copper. This information is essential because depending on the type of metal and corrosion products, the green protocol that can be applied to restore or preserve the product also changes. **F**ibula seems to be part of the collection of fibulas found in the tomb 11 of Madonnelle necropolis it was

contained in a Corinthian amphora in an infant burial. Using astragalus as a playing piece and depositing it in the tomb was a Greek practice in this period. So, the presence of the fibulas inside the tomb gives the certainty that it belongs to a child. The use of the fibula is a characteristic of the Greek period (Verger, 2014). A similar fibula was also found in Albania, characterized from a chemical-physical point of view using OM, and SEM-EDS techniques. XRF analysis showed similar elements to ours that this fibula was made of a copper-tin binary alloy (Cajaj, O, 2016).

The correct chemical composition was also detected from the analyses carried out on the lancet, an artifact that had the function of a surgical scalpel. According to the museum literature, it should be entirely made of iron, information which is partly true since the blade of the lancet is of iron. Still, XRF provided precise indications on the chemical composition of the lancet handle, reporting the presence of copper, zinc, iron, lead, and tin and therefore revealing the presence of a binary alloy copper-zinc (Cu-Zn) which forms brass. This result was enjoyable as the lancet's presumed dating was considered the 4th-2nd century BC. Still, the period in which brass appeared in the Balkan area dates back to the end of the 2nd century BC (Bursak et al., 2022), in which the Western Roman Empire annexed the Balkan region. Therefore, it is possible to think that the artifact in question arrived in the Policoro (MT) area when began the trade routes between the two territories, now part of the same empire.

The metal finds granted by the Museum for this study were in a severe state of alteration due to corrosion. The inscriptions that described these objects in the Museum were not always accurate because they were based solely on visual observation. Optical microscope analysis and, even more profoundly, the spectra obtained with non-destructive instrumental

methods based on X-rays have returned a reality that is sometimes different from the visual one. By applying these instrumental methods, it will be possible to make a more informed choice of technologies to preserve and conserve perishable archaeological resources.

Author Contributions: Conceptualization: LS, GR; Methodology: GR, LS, SG, GT, EM; Validation: GR LS, GT, EM, formal analysis: NS; investigation: LS, GR, GT, EM, NS; data curation: LS, GR, GT, EM; writing—original draft preparation, NS, LS, GR; writing—review, and editing: LS, GR, GT, EM; supervision: GR, LS. All authors have read and agreed to the published version of the manuscript.

ACKNOWLEDGEMENTS

This work was supported by the "Industrial Doctorate 4.0" scholarship for the International Doctorate "Applied Biology and Environmental Protection" of Basilicata University. We thank the Superintendence of Basilicata and the Siritide Museum for allowing the analyzes of metal exhibits in the museum. XRPD laboratory at the Dipartimento di Scienze della Terra and Geoambientali, University of Bari "Aldo Moro", was funded by PONa3_00369 "Laboratorio per lo Sviluppo Integrato delle Scienze e delle TEcnologie dei Materiali Avanzati e per dispositivi innovativi (SISTEMA)". The authors especially thank Fausto Langerame and Lorenzo Montinaro of Basilicata University for their support and technical cooperation.

REFERENCES

Aceto M., (2005). Handout for the Analytical Chemistry Course for Cultural Heritage, pp. 56-57.

Ali A., Chiang YW., Santos RM., (2022). X-ray Diffraction Techniques for Mineral Characterization: A Review for Engineers of the Fundamentals, Applications, and Research Directions Minerals, 12(2), 205. https://doi.org/10.3390/min12020205

Artioli G. (2010) An Introduction to the Application of Materials Science to Archaeometry and Conservation Science. Oxford Univ. Press, New York. *Scientific Methods and Cultural Heritage,* Vol. 9, p. 553.

Avilia F., (1980). Metals and metal alloys. *MTC Ancient Metals,* pp. 3-4.

Balassone G., Mercurio M., Germinaro C., Grifa C., Villa I. M., Dimaio G., Scala S., de' Gennaro R., Petti C., del Re M. C., Langella A., (2018*).* Multi-analytical characterization and provenance identification of protohistoric metallic artifacts from Picentia-Pontecagnano and the Sarno valley sites, Campania, Italy. *Measurement,* Vol. 128, pp. 104-118.

Bernard M. C., Joiret S., (2003). Understanding corrosion of ancient metals for the conservation of cultural heritage. *Electrochimica Acta* 54(22), pp. 5199-5205

Bouchard M, Smith D. C., (2003). Catalogue of 45 reference Raman spectra of minerals concerning research in art history or archaeology, especially on corroded metals and coloured glass. *Spectrochimica Acta, Vol 59,* pp. 2247-2266.

Briggs D., (1990). Practical surface analysis. *Auger X-Ray Photoelecton Spectrosc*., 1, pp. 151–152.

Brocchieri, J., Scialla, E., Manzone, A., Graziano, G.O., D'Onofrio, A. and Sabbarese, C. (2022) The gilding technique on lead objects of The Royal Palace in Caserta (Italy) studied by pXRF. *Mediterranean Archaeology and Archaeometry*, Vol. 22, No 1, pp. 29-43.

Bursak D., Danielisova A., Magna T., Pajdla P., Mikova J., Rodovska Z., Strnad L., Trubac J., (2022). Archaeometric perspecgtive on the emergence of brass north of the Alps around the turn of the Era. *Scientific reports,* Vol. 12, p. 374.

Cabibbo M., (2018). Non-ferrous metals and alloys. *Società editrice Esculapio.*

Çakaj O., Dilo T., Schmidt G., Civici N., Stamati F. (2016). Fibula and snake bracelet from albania. A case study by OM, SEM-EDS and XRF. *Scientific Culture*, 2 (2), pp. 9-18

Campanella L., Colacchi Alessandri O., Ferretti M., Plattners S. H., (2009). The effect of tin on dezincification of archaeological copper alloys. *Corrosion Scienze,* Vol. 51, pp. 2183-2191.

Chiavari C., Colledan A., Frignani A., Brunoro G. (2006). Corrosion evaluation of traditional and new bronzes for artistic castings. *Materials Chemistry and Physics,* Vol.95, Issues 2–3, pp. 252–259.

Corsi J., Grazzi F., Lo Giudice A., Re A., Scherillo A., Angelici D., Allegretti S., Barello F., *(*2016). Compositional and microstructural characterization of Celtic silver coins from northern Italy using neutron diffraction analysis. *Microchemical Journal,* Vol 126, pp. 501-508.

Electrochimica Acta, Vol. 54, pp. 5199-520.

Figueiredo E., Valario P., Arau jo M. F., Senna-Martinez J. C., (2007). Micro-EDXRF surface analyses of a bronze spear head: Lead content in metal and corrosion layer. *Nuclear Instruments and Methods in Physics Research,* Vol. 580, pp. 725- 727.

Frost R. L., (2003). Raman spectroscopy of selected copper minerals of significance in corrosion. *Spectrochimica Acta,* Vol. 59, pp. 1195-1204.

Giumilia-Mair A., (2005). Archaeometallurgy: the contribution of mineralogy. *Industr. and Methods in Phisics Research,* Vol 239, pp. 35-43.

Iacopini S., (2012). Analytical investigations on silver artifacts of the archaeological site of Classe (Ravenna). *ACADEMIA.*

Ingo G.M., De Caro T., Ricucci C., Angelini E., Grassini S., Balbi S., Bernardini P., Salvi P., Bousselmi P., Ciringinoglu A., Gemer A., Gouda V. K., Al Jarrah O., Khossroff O., Mahdjoub Z., Al Saad Z., El-Saddik W., Vassilou P. (2006). Uncommon corrosion phenomena of archaeological bronze alloys. *Appl. Phys,* Vol 83, pp. 581-588.

ISO (1999). Corrosion of metals and alloys - *Basic terms and definitions.*

IUPAC (2014). Compendium of Chemical Terminology - Gold Book. *International Union of Pure and Applied Chemistry.*

Kousouni CK, Gkanetsos T., Panagopoulou A., (2021). Non – destructive XRF analysis of metallic objects from benaki museum of islamic art. Scientific culture, 7(2), pp. 69-79

Kylafi, M., Katakos, A., Boyatzis, S., Palamara, E. and Zacharias N. (2017) Characterisation and Analysis of Metallic Artefacts from the Pylos Archaeological Museum, *STAR: Science & Technology of Archaeological Research*, Vol. 3, No. 2, pp. 161-168

Lekbach, Y., Liu, T., Li, Y., Moradi, M., Dou, W., Xu, D., Smith, J.A. and Lovely, D.R. (2021) Microbial corrosion of metals: The corrosion microbiome. *Adv Microb Physiol.* Vol 78, pp. 317-390. DOI: 10.1016/bs.ampbs.2021.01.002.

Liritzis I., Zacharias N., Papageorgiou I., Tsaroucha A., Palamara E., (2018). Characterisation and analyses of museum objects using pXRF: An application from the Delphi Museum, Greece. *Studia Antiqua et Archaeologica*, 24(1), pp. 31–50.

Longman J., Veres D., Finsinger W., Ersek V., (2017). Exceptionally high levels of lead pollution in the Balkans from the Early Bronze Age to the Industrial Revolution. *PNAS 115(25):E5661-E5668. doi: 10.1073/pnas.1721546115*

MacLeod I.D., (1991). Identification of corrosion products on non-ferrous metal artifacts recovered from shipwrecks. *Studies in Conservation,* Vol 36, pp. 222-234.

Mata, A.L., Carneiro, A., Neto, M.M.M., Proneca, L.A., Salta, M.M.L., Mendoca, H., Fonseca, I.T.E. (2010). Characterisation of five coins from the archaeological heritage of Portugal. *Journal of Solids State electrochemistry*, Vol. 14, 495–503.

Matthew, J. (2004). Surface Analysis by Auger and X-ray Photoelectron Spectroscopy; Briggs, D., Grant, J.T., *Eds.; IMPublications: Chichester, UK; SurfaceSpectra: Manchester*, UK, 2004; p. 900.

Mazzeo R., Prati S., Quaranta M., Sciutto G. (2012). An overview of analytical techniques and methods for the study and preservation of artistic and archaeological bronzes. *Mediterranean Archaeology and Archaeometry*, 12 (2), pp. 261-271.

Mircea, O., Sandu, I., Vasilache, V., Sandu, IG (2012) A study on the deterioration and degradation of metallic archaeological artifacts. *International Journal of Conservation Science*, Vol. 3, No. 3, pp. 179-188.

Moropolou A., Labropoulos KC., Delegou ET., Karoglou M., Bakolas A., (2013). Non-destructive techniques as a tool for the protection of built cultural heritage. *Constructions and Building Materials,* Vol. 48, pp. 1222-1239.

Muşkara Ü., Aydýn, M. (2022). Elemental analysis of pre-Pottery Neolithic B copper finds from Gre Filla. *Mediterranean Archaeology and Archaeometry*, Vol. 22, No 1, pp. 1-14

Parmeggiani G. (2003). L' εὑρεῖν senza σαφές: Thucydides and knowledge of the past. *Ancient society* Vol. 33, pp. 235-283.

Pescatore T., Pieri P., Sabato L., Senatore M. R., Gallicchio S., Boscaino M., Cilumbriello A., Quarantiello R. & Capretto G. (2009). Stratigraphy of the Pleistocene-Holocene deposits of the coastal area of Metaponto between Marina di Ginosa and the Cavone Torrent (Southern Italy): Geological Map at a scale of 1:25,000. *Il Quaternario,* Vol. 22, Issue 2, pp 307-323.

Pintori G., Cattaruzza E., (2022), XPS/ESCA on glass surfaces: A useful tool for ancient and modern materials. *Optical Materials:X,* Vol 13, pp. 1-40.

Rifai M., Elshahawi A., and Hamid ZA., (2016). Technical and conservation study of a Bronze mirror from Aniba, lower Nubia, Egypt. *Scientific Culture*, Vol. 9 (1), pp. 21-35

Robbiola L., Tran T.T.M., Dubot P., Majerus M., Rahmouni K., (2008). Characterisation of anodic layers on Cu–10Sn bronze (RDE) in aerated NaCl solution. *Corrosion Science,* Vol. 50, Issue 8, pp 2205–2215.

Sabato L., Longhitano S., Cilumbriello A., Gioia D., Spalluto L., Kalb C. (2011). Sedimentological study and marine- coastal dynamics of the Bosco Pantano di Policoro littoral system (Basilicata, southern Italy). *Rendiconti Online Società Geologica Italiana,* Vol. 17, pp. 161-168.

Salem Y., and Allah EA., (2021). Archaeometallurgical investigation, manufacturing technique and conservation processses of a coptic/byzantine age hoard of unstruck coins flans. *Scientific Culture*, 7 (3), pp. 65-76

Stanjek H. and Häusler W., (2004). Basics of X-ray Diffraction. *Hyperfine Interactions*, Vol.154, pp. 107-119

Verger S. (2014). Kolophon et Polieion: A propos de quelques obets métalliques archaiques de Policoro*, In: SIRIS, studi e ricerche della scuola di specializzazion in beni archeologici di matera No* 14, Università degli Studi della Basilicata Scuola di Specializzazione in Beni Archeologici di Matera, Italy, pp. 15-41.

Videla H.A., (2002). Prevention and control of biocorrosion. *International Biodeteroration and Biodegradation*, 49 (4) pp. 259- 270.